(This article was presented to the 28th National Chemistry Congress and submitted to JOTCSA as a full manuscript)

Photocatalytic Activities of Ag^+ Doped ZIF-8 and ZIF-L Crystals

Hüsnü Arda Yurtsever[a1], Melis Yağmur Akgünlü[a], Tuğçe Kurt[a], Ali Semih Yurttas[a], Berna Topuz[a*]

Ankara University, 06100, Ankara, Turkey

Abstract: Zeolitic imidazolate framework (ZIF) based metal organic framework (MOF) photocatalytsts were prepared and the effect of silver (Ag^+) doping on the photocatalytic activity of ZIF-8 and ZIF-L crystals was investigated. Ag^+ doped ZIF-8 and ZIF-L crystals were prepared and their activities in the photocatalytic removal of methylene blue (MB) dye under UV irradiation were determined for the first time in the literature. Doped ZIF-8 and ZIF-L crystals showed better photocatalytic activities compared to the undoped crystals. Almost 100% of MB was removed with 5 mole% Ag^+ doped ZIF-8 in 40 min. The magnitude of the calculated 2nd order reaction rate constants changed in the order of 5%>10%>2%>1%>undoped ZIF-8. The photocatalytic activity decreased beyond 5 mole% doping level since Ag^+ ions may have segregated due to a possible solid state solubility limit of Ag^+ ions in the crystal lattice of ZIF-8. ZIF-L crystals possessed a lower photocatalytic activities compared to ZIF-8 crystals.

Keywords: Photocatalysis; metal-organic framework; ZIF-8; ZIF-L, doping.

Submitted: July 4, 2016. **Revised:** July 28, 2016. **Accepted:** September 01, 2016.

Cite this: Yurtsever H, Akgünlü M, Kurt T, Yurttaş A, Topuz B. Photocatalytic Activities of Ag+ Doped ZIF-8 and ZIF-L Crystals. JOTCSA. 2016;3(3):265–80.

DOI: 10.18596/jotcsa.10970.

* Corresponding Author. E-mail: topuzb@ankara.edu.tr.

[1] Current Address: Adana Science and Technology University, Adana, Turkey.

INTRODUCTION

Photocatalysis is expected to contribute to the solution of environmental problems such as water and air pollution in the near future. The design of photocatalysts with high electron-hole generation rates, high surface areas and high light absorption capacities is crucial in producing sustainable and cost-effective photocatalytic processes. Titania, zirconia, copper oxide, zinc oxide, and iron oxide are widely used photocatalysts which have good light absorption capacities with moderate surface areas depending on the synthesis conditions. Intense research and advances in nanoscience and nanotechnology improved the preparation techniques and expanded the application area of nanostructured photocatalytic materials. Fujishima and Honda conducted the pioneering studies in 1970s to produce renewable energy via photocatalytic processes by using solar energy (1, 2). Since then many photocatalytic materials were prepared to be used in various photocatalytic processes. There are many examples in the literature and there is a huge variety of photocatalytic materials to be used in many different photocatalytic processes (3).

In the last decade, metal organic frameworks (MOFs) have been used in photocatalytic applications due to their very high surface areas up to 3000s of m^2/g, tunable ligand/metal clusters, and adequate light absorption capacities. MOFs are the porous crystalline hybrid materials with well-ordered pores and cavities which are mostly used in adsorption, catalysis, and separation processes where the molecular sieving and the preferential adsorption is important. Their use in photocatalysis is promising since they have high porosity and surface areas compared to oxide photocatalytic materials prepared at high temperatures. However, thermal and chemical stability of MOFs during the photocatalytic reaction is still an important issue.

Since MOFs contain organic linker with inorganic subunits they can show semiconducting properties with tunable band gap. Diversity on the metal ions and the organic linkers, and easily controlled synthesis steps make MOF materials with tailorable capacity to absorb light. Although these desirable properties open exciting opportunities to use them in photocatalytic applications, comprehensive studies on the use of MOF crystals in photocatalytic processes has not been explored widely.

Zeolitic imidazole frameworks (ZIFs) are the sub-family of MOFs, which can be synthesized by solvothermal/hydrothermal, and microwave assisted reactions at temperatures in the 298-423 K range. ZIF-8 and ZIF-L are the topologically isomorphs of

zeolites with tetrahedrally coordinated zinc metal and imidazole rings (4, 5) and they can be easily synthesized in aqueous medium at room temperature. ZIF-8 has SOD topology exhibiting 3D structure with cages 11.6 Å in diameter, which are accessible through 3.4 Å windows. Leaf-shaped 2D ZIF-L crystals have the same building units with those for ZIF-8 and have cushion-shaped cavity with dimensions of 9.4 Å x 7.0 Å x 5.3 Å (6). These materials have high surface area and high CO_2 adsorption capacities. These properties make them promising photocatalytic materials to be used in artificial photosynthesis (CO_2 photoreduction).

Photocatalytic removal of methylene blue (MB) dye was performed successfully under UV light irradiation with pure ZIF-8 nanocrystals by Jing *et al.* (7). They reported ~85% degration of MB with undoped ZIF-8 crystals under UV light irradiation. After 3.5 h, the conversion of MB was reported as 50% for polyoxometalate (POM) based MOF type photocatalyst (8).

Studies on photocatalytic applications have shown that combining ZIF-8 with semiconductors having different band structures or introducing impurity levels can increase light absorption capability, decrease the recombination rate of electron-hole pairs; hence increase the photocatalytic activity.

The photocatalytic activities of TiO_2, Zn_2GeO_4, and ZnO were increased by the incorporation of a ZIF-8 layer (10-12). Benzyl alcohol was oxidized with Au nanoparticles encapsulated ZIF-8 nanocrystals (13) under visible light. Ag^+/AgCl was synthesized on ZIF-8 nanocrystals with different weight ratios and their photocatalytic activities in the removal of RhB dye were evaluated (14). Ni substitute ZIF-8 photocatalysts were prepared for alcohol sensing and photocatalytic removal of methylene blue activities of the prepared photocatalysts were evaluated under visible light illumination (15). Studies on Ag^+ doped ZIF-8 and ZIF-L including their photocatalytic performances are currently limited to the best of our knowledge.

In this study, Ag^+ doped ZIF-8 nanocrystals with different Ag^+ contents were prepared and their photocatalytic activities under UV light irradiation towards methylene blue dye removal were evaluated. Doped and undoped ZIF-L crystals were also prepared and their activities were compared with those of ZIF-8 crystals for the first time in the literature.

MATERIALS AND METHODS

Materials

Zinc nitrate hexahydrate (98%, Aldrich), silver nitrate (99+%, Alfa Aesar), 2-methylimidazole (Hmim, 99%, Aldrich) and methanol (≥99.9%, Aldrich) were used as received without any further purification. DI water (18.2 MΩ cm) was also used in the synthesis of ZIF-L crystals.

Synthesis of Undoped/Doped ZIF 8 and ZIF-L Crystals

Undoped ZIF-8 crystals were synthesized as reported before (16). Methanol (47.52 g) solutions of $Zn(NO_3)_2.6H_2O$ (1.286 g) and Hmim (2.811 g) were prepared separately and then mixed by dropwise addition of the Hmim solution to the Zn^{2+} solution. The synthesis solutions were stirred at room temperature for 1.5 h. The crystals were separated by centrifugation (8000 rpm, 15 min) and washed with methanol (3 × 30 mL). The obtained white powders were dried at 80ºC overnight before characterization and photocatalytic experiments. Doped ZIF-8 crystals were synthesized by following the same route. $AgNO_3$ was added to the Zn^{2+} containing solution for the preparation of Ag^{+} doped ZIF-8 crystals. $AgNO_3$ amount was calculated by keeping the total metal amount as 1 mol. The Metal:Hmim:MeOH molar ratios were 1:8:700 for the undoped/doped ZIF-8 crystals.

Undoped ZIF-L crystals were synthesized as described elsewhere (5,6). Aqueous (50 mL) solutions of $Zn(NO_3)_2.6H_2O$ (0.662 g) and Hmim (1.642 g) were mixed by the dropwise addition of the Zn^{2+} solution to the Hmim solution. The mixture was stirred at room temperature for 4 h and then subjected to centrifugation at 10000 rpm for 20 min (5). The obtained white powder was washed with water three times. The final powder product was stored in an oven at 105 °C. Doped ZIF-L crystals were synthesized by following the same route. $AgNO_3$ was added to the Zn^{2+} containing solution for the preparation of Ag doped ZIF-L crystals which was the same as in the synthesis of doped ZIF-8 crystals. The Metal:Hmim:H_2O molar ratios were 1:8:2241 for the undoped/doped ZIF-L crystals.

Characterization of ZIF-8 and ZIF-L Crystals

The prepared ZIF-8 and ZIF-L crystals were characterized by using X-Ray Diffraction (XRD, Rigaku Ultima-IV) equipment with monochromated high-intensity (λ=1.54 Å) CuKα radiation. The scanning step size and time were 0.02 (º) and 411.2 (s), respectively, in

the 5 and 80° 2theta range. Morphology and particle sizes were characterized by Scanning Electron Microscopy (SEM, QUANTA 400F) in the 20-50 kx magnification range.

Photocatalytic Removal of Methylene Blue

Photocatalytic experiments were conducted by using a home-made inner-irradiated photoreactor. The prepared powders (0.05 g) were dispersed in 10 ppm, 60 mL methylene blue solution. The suspensions were kept in an ultrasonic bath for 5 min to provide well dispersion. A 9W UV lamp was used as the irradiation source. Samples were withdrawn from the suspension by using a syringe with 10-minute time intervals. The samples were centrifuged and analyzed with a UV-Vis Spectrophotometer (Shimadzu UV-1600). The spectra of the samples were recorded in the 300-800 nm range and 664 nm (maximum absorption wavelength for methylene blue) was selected for the calculation of dye concentration. Methylene blue removal (%) was calculated by using the relation, MB removal % = 100-(C/C_0)*100, where C is the concentration of the sample and C_0 is the initial methylene blue concentration. The data were fitted to second order reaction rate expression, $1/C_0-1/C = -k*t$, where k is the second order reaction rate constant and t is time.

RESULTS AND DISCUSSION

Characterization of ZIF-8 and ZIF-L Crystals

XRD patterns of undoped/10% Ag^+ doped ZIF-8 and ZIF-L crystals are given in Figure 1 along with the reference simulated XRD patterns (4, 5). The peak positions belonging to the prepared crystals coincide with reference peak positions as shown in the figure, which also showed that ZIF-8 and ZIF-L crystals were successfully synthesized. Although random orientation was observed for the powder samples, XRD patterns of both undoped and 10% Ag^+ doped ZIF-L exhibit intensity ratios different than that of the reference. Since ZIF-L has a 2-D layer network along the *ab* plane stacking along the *c* direction (6), packing of 2-D morphology may affect the orientation for the powder. The results given in Figure 1 also show that the presence of Ag^+ ion in the synthesis medium did not cause any framework change during the crystallization. The relative crystallinities have decreased upon addition of Ag^+ ion to the both structures. There were no peaks of impurity phases other than ZIF-8 phase in the XRD pattern of 10 mole % Ag^+ doped ZIF-8 and ZIF-L. This indicated that no Ag^+ phases were formed during the synthesis. Ag^+

ions may substitute Zn^{2+} ions, accommodate in the interstitial voids of ZIF-8 lattice or segregate as small clusters with the sizes which are out of XRD detection limit.

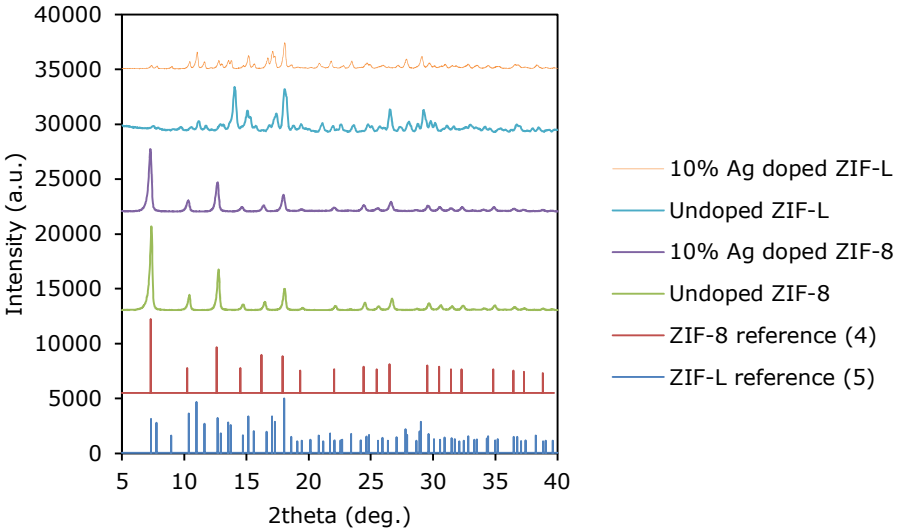

Figure 1. XRD patterns of the prepared crystals.

SEM images of undoped/10% Ag^+ doped ZIF-8 and ZIF-L crystals are shown in Figures 2 and 3, respectively. The size of the synthesized ZIF-8 crystals was estimated as ~60 nm for undoped ZIF-8 crystals and the size slightly decreased with Ag^+ doping and the SEM images also indicated that individual undoped/doped ZIF-8 crystals were successfully synthesized. The SEM images of ZIF-L crystals indicated that 2-dimensional crystals (5 μm x 2 μm) with a thickness of ~100 nm were successfully synthesized (Figure 3a). The dimensions of the doped ZIF-L crystals were estimated to be 3 μm x 1 μm with the same thickness. SEM-EDX analysis of the 10% Ag^+ doped ZIF-8 and ZIF-L crystals were also performed. SEM-EDX indicated that silver clusters were not formed at relatively high doping levels (10%) and Ag^+ ions were well dispersed in the crystalline structure (data not shown here).

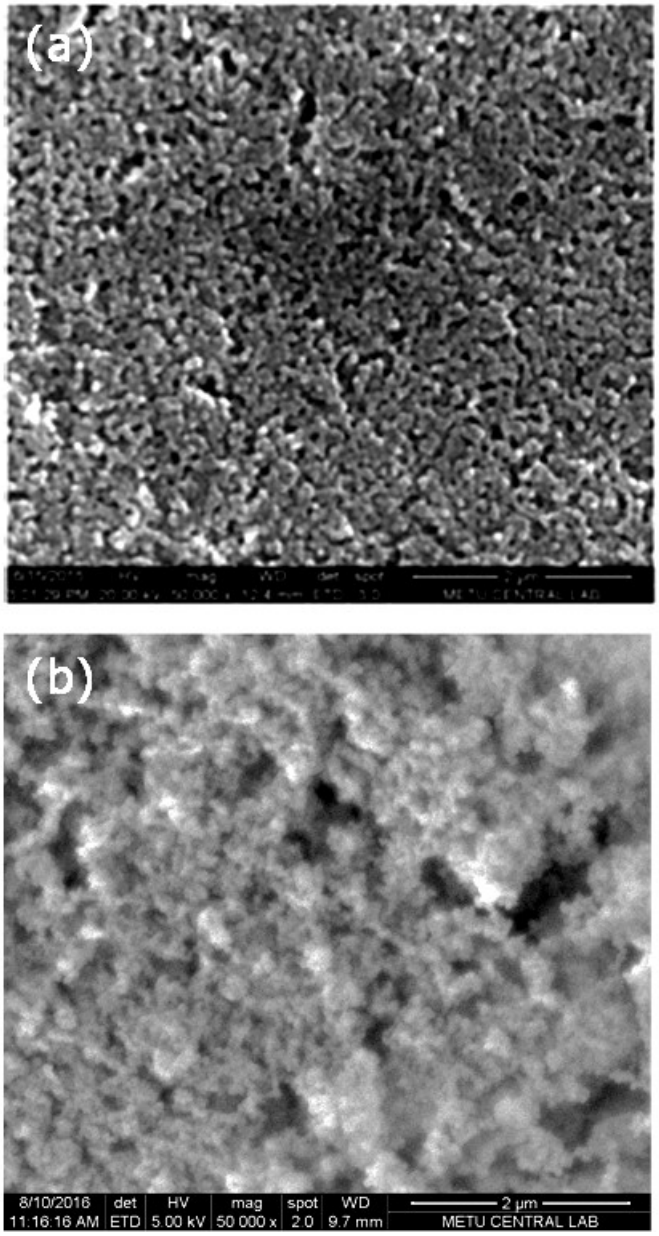

Figure 2. SEM images of (a) undoped and (b) 10% Ag^{+} doped ZIF-8 crystals.

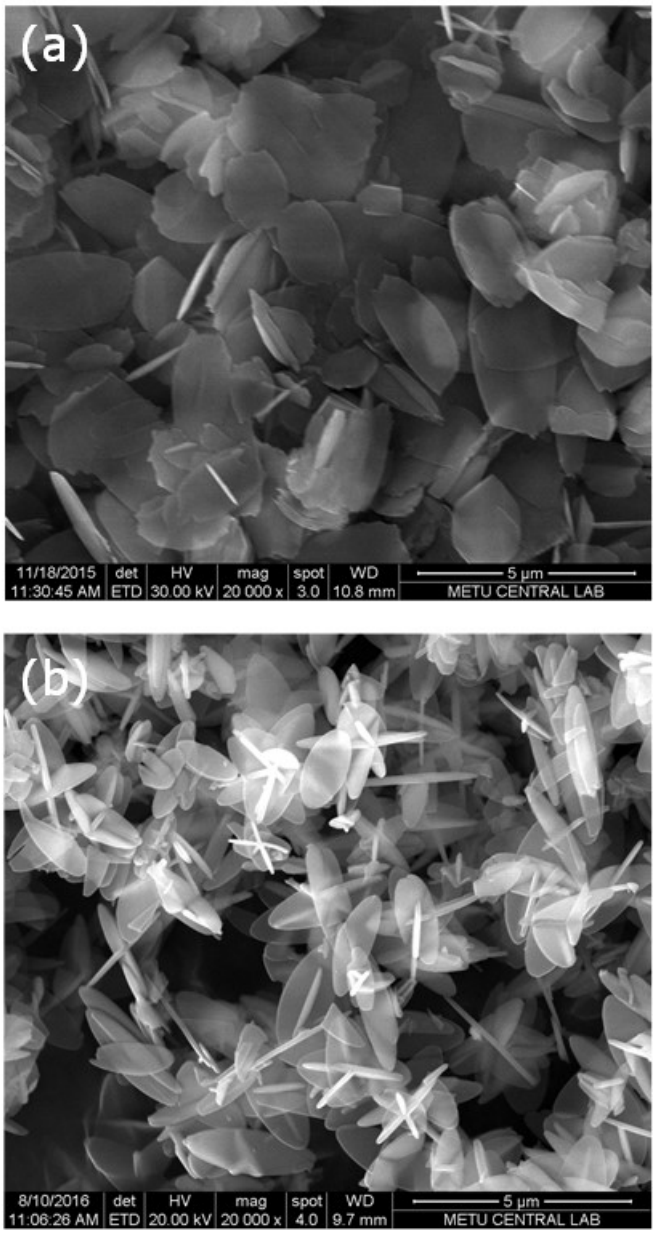

Figure 3. SEM images of (a) undoped and (b) 10% Ag^+ doped ZIF-L crystals.

Photocatalytic Removal of Methylene Blue

The photocatalytic activities of the prepared ZIF-8 and ZIF-L crystals in the removal of methylene blue under UV irradiation were determined. 4% MB was photocatalytically decomposed without ZIF-8/ZIF-L catalyst upon UV-light irradiation for 40 min. Time-dependent MB removal (%) and the plots of $1/C-1/C_0$ vs time obtained with ZIF-8 crystals are given in Figures 4 and 5. Methylene blue was nearly 100% removed in 40 min with 5 mole % Ag^+ doped ZIF-8. In comparison with the previously reported

performances, 5%-Ag^+ doped ZIF-8 exhibited better photocatalytic activity towards MB (7-9).

Undoped and 1 mole% Ag^+ doped ZIF-8 crystals showed the lowest activities towards the photocatalytic removal of methylene blue (Figure 4). Ag^+ doping increased the photocatalytic activity of ZIF-8 for all doping levels. Doping may have increased the light absorption capability and decrease the recombination rate of electron-hole pairs which may lead to an increase in the photocatalytic activity of ZIF-8. The photocatalytic activity decreased beyond a certain doping level (5%) since Ag^+ ions may have segregated due to a possible solid state solubility limit of Ag^+ ions in the crystal lattice of ZIF-8. It is possible for Ag^+ ions to substitute for the Zn^{2+} ions in the lattice or accommodate in the interstitials. Segregation, hence, would block the reactive surface of ZIF-8, which results in a decrease in the photocatalytic activity.

The photocatalytic removal of methylene blue kinetics was best fitted to 2nd order reaction rate expression. The plots of $1/C-1/C_0$ vs time are given in Figure 5. The magnitude of the calculated 2nd order reaction rate constants changes in the following order: %5>10%>2%>1%>undoped ZIF-8 (Table 1). A pseudo-first-order kinetics was reported for MB degradation over the ZIF-8 undoped photocatalyst (7). Differences in kinetics for MB removal might be due to the smaller particle size of ZIF-8 (60 nm) which may affect the adsorption rate of MB.

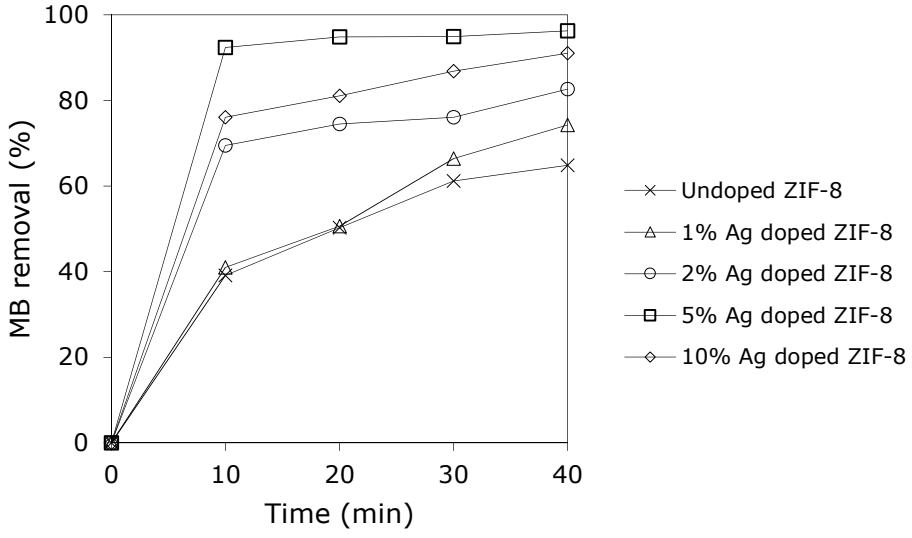

Figure 4. Time dependent MB removal (%) of undoped/doped ZIF-8 crystals.

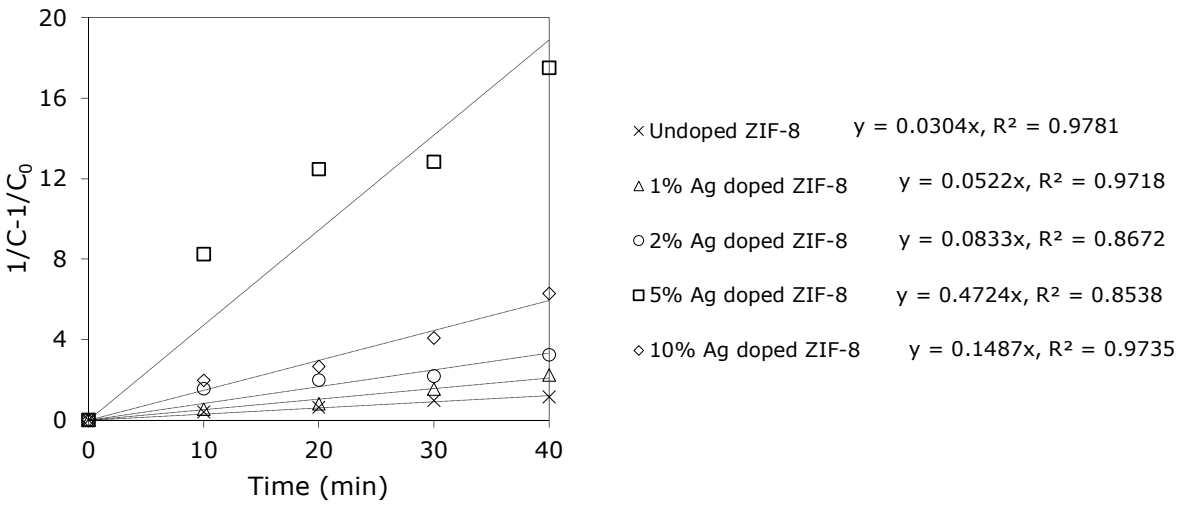

Figure 5. Reaction kinetics of undoped/doped ZIF-8 crystals.

The photocatalytic activities of the undoped/5 mole% Ag^+ doped ZIF-L crystals were also determined. Time dependent MB removal (%) and the plots of $1/C-1/C_0$ vs time obtained with undoped/doped ZIF-L (and the corresponding values for ZIF-8 for comparison) are given in Figures 6 and 7, respectively. Methylene blue removal activities of ZIF-L crystals were very low when compared to those of ZIF-8 crystals. ZIF-L and ZIF-8 are both composed of Zn metal center and imidazole linker in their structures but differ in crystal morphology. Compared to ZIF-8, ZIF-L has a lower porosity and surface area (N_2 adsorption at 77K) (6). Therefore, the significantly lower surface area of ZIF-L could be the reason for low photocatalytic activities. Ag^+ doped ZIF-L crystals possessed slightly higher photocatalytic activity compared to the undoped ZIF-L crystals. Ag^+ doping may increase the light absorption capability and decrease the recombination rate of electron-hole pairs, hence increase the photocatalytic activity of ZIF-L crystals.

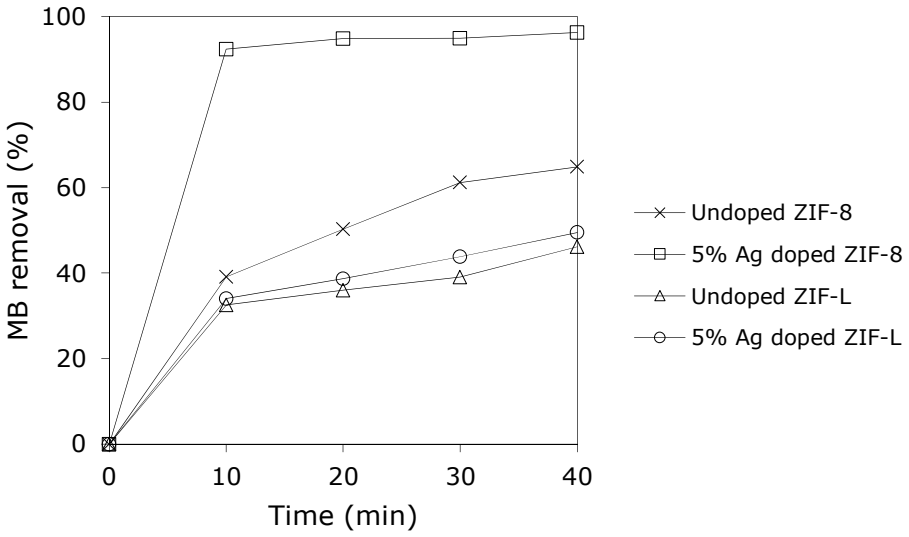

Figure 6. Time dependent MB removal (%) of undoped/doped ZIF-8 and ZIF-L crystals.

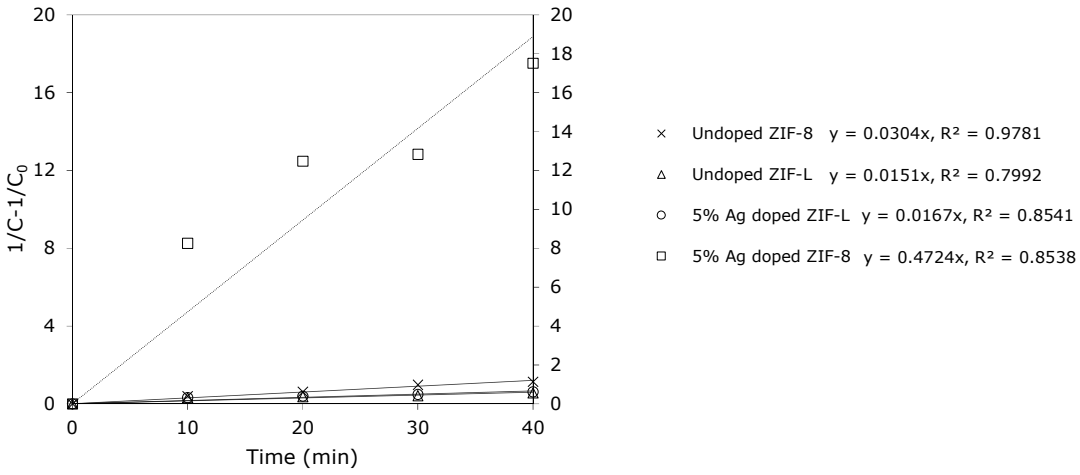

Figure 7. Reaction kinetics of undoped/doped ZIF-8 and ZIF-L crystals.

UV-Vis absorption spectra of the MB solution during the reaction under UV irradiation in the presence of 5%-Ag^+ ZIF-8 and 5%-Ag^+ ZIF-L are given in Figure 8(a), and Figure 8(b), respectively. The results shown in this figure, indicated that both crystals exhibit different behavior towards photocatalytic decomposition of MB. MB concentration decreased dramatically within 10 min in the presence of 5%-Ag^+ ZIF-8. However, the absorbance of MB decreased gradually with the increase of irradiation time, and 49% of MB was removed after 40 min under UV irradiation in the presence of 5%-Ag^+ ZIF-L.

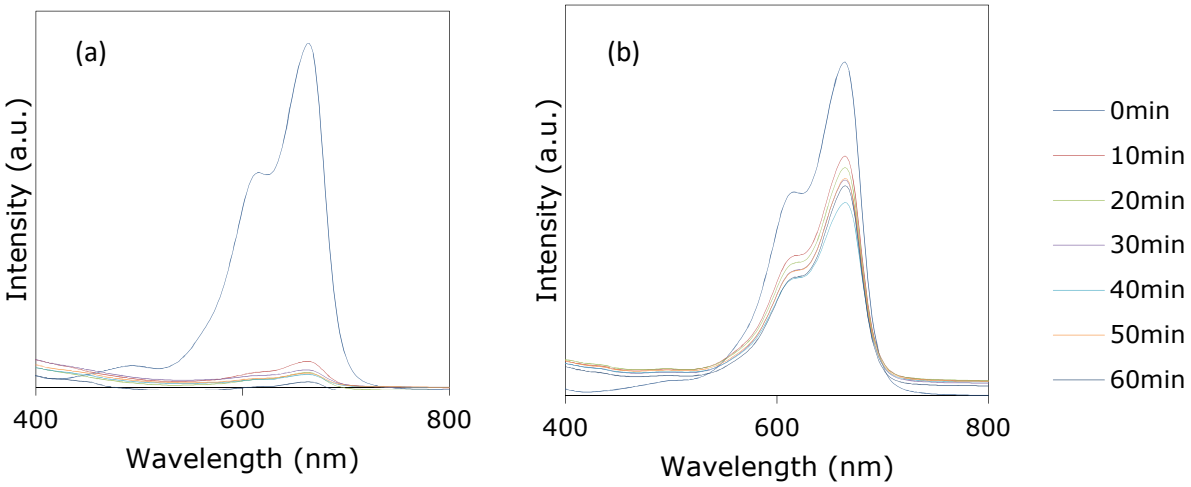

Figure 8. UV-Vis absorption spectra of the MB solution during the reaction under UV irradiation in the presence of (a) 5%-Ag^{2+} ZIF-8, (b) 5%-Ag^{2+} ZIF-L.

MB adsorption experiments (without UV light) were also conducted in order to determine whether the MB removal was achieved by adsorption or photocatalysis. MB removal % of the prepared photocatalysts by adsorption and photocatalysis in 40 minutes are given in Figure 9. The results have shown that the prepared undoped/doped ZIF-8 and ZIF-L crystals are photocatalytically active materials. MB adsorption was determined to be the highest for 2% Ag^{+} doped ZIF-8 crystals. These results also supported that 5% Ag^{+} doped ZIF-8 crystals have the highest photocatalytic activity since the photocatalytic removal % and adsorption % difference is more compared to the other crystals. Reusability test was conducted with 5% Ag^{+} doped ZIF-L crystals. MB removal % slightly decreased from 49% to 42% in the second run.

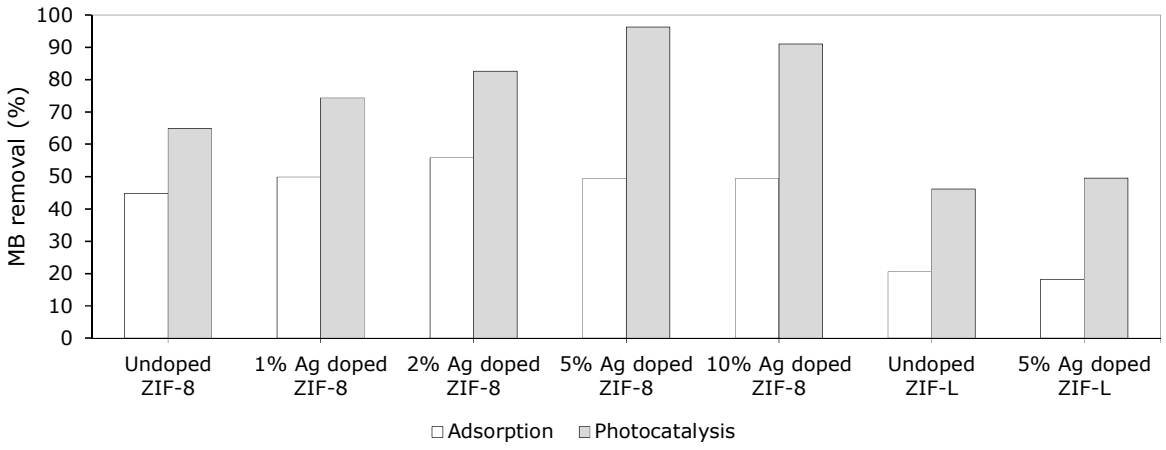

Figure 9. MB removal by adsorption and photocatalysis.

Table 1. Calculated 2nd order reaction rate constants.

Photocatalyst	**2nd order reaction rate constant (1/ppm.min)**
Undoped ZIF-8	0.0304
1% Ag^+ doped ZIF-8	0.0522
2% Ag^+ doped ZIF-8	0.0833
5% Ag^+ doped ZIF-8	0.4724
10% Ag^+ doped ZIF-8	0.1487
Undoped ZIF-L	0.0151
5% Ag^+ doped ZIF-L	0.0167
10% Ag^+ doped ZIF-L	0.0196

Overall, we report that Ag^+ doping in certain amount into the ZIF-8 and ZIF-L crystals facilitated the MB removal under UV-light irradiation. This allowed almost complete removal of MB for ZIF-8 crystals. These findings may contribute to the development of simple, environmentally friendly, and highly efficient photocatalyst for degradation of MB. Further research on influence of parameters on degradation kinetics and detailed characterization of these promising photocatalyst may significantly develop our understanding of photocatalytic mechanism towards MB degradation.

ACKNOWLEDGMENTS

This study was supported by The Scientific and Technological Research Council of Turkey (TUBITAK) within the context of 214M012 project.

REFERENCES

1. Fujishima A, Honda K. Electrochemical Photolysis of Water at a Semiconductor Electrode. Nature. 1972;238(5358):37-8: DOI: 10.1038/238037a0.

2. Inoue T, Fujishima A, Konishi S, Honda K. Photoelectrocatalytic reduction of carbon dioxide in aqueous suspensions of semiconductor powders. Nature. 1979;277(5698):637-8: DOI: 10.1038/277637a0.

3. Hoffmann MR, Martin ST, Choi W, Bahnemann DW. Environmental Applications of Semiconductor Photocatalysis. Chemical Reviews. 1995;95(1):69-96: DOI: 10.1021/cr00033a004.

4. Schejn A, Aboulaich A, Balan L, Falk V, Lalevee J, Medjahdi G, et al. Cu^{2+}-doped zeolitic imidazolate frameworks (ZIF-8): efficient and stable catalysts for cycloadditions and condensation reactions. Catalysis Science & Technology. 2015;5(3):1829-39: DOI: 10.1039/C4CY01505C.

5. Zhong Z, Yao J, Chen R, Low Z, He M, Liu JZ, et al. Oriented two-dimensional zeolitic imidazolate framework-L membranes and their gas permeation properties. Journal of Materials Chemistry A. 2015;3(30):15715-22: DOI: 10.1039/C5TA03707G.

6. Chen R, Yao J, Gu Q, Smeets S, Baerlocher C, Gu H, Zhu D, Morris W, Yaghi O, Wang H. A two-dimensional zeolitic imidazolate framework with a cushion-shaped cavity for CO_2 adsorption. Chem. Commun. 2013;49:9500-02: DOI: 10.1039/C3CC44342F.

7. Jing H-P, Wang C-C, Zhang Y-W, Wang P, Li R. Photocatalytic degradation of methylene blue in ZIF-8. RSC Advances. 2014;4(97):54454-62: DOI: 10.1039/C4RA08820D.

8. Wang X, Han N, Lin H, Luan J, Tian A, Liu D. A novel 3D metal–organic framework constructed from monosubstituted Keggin chains and metal–carboxylate chains. Inorg. Hem. Commun. 2014;42:10-14: DOI: 10.1016/j.inoche.2014.01.012.

9. Yu B, Wang F, Dong W, Hou J, Lu P, Gong J. Self-template synthesis of core–shell ZnO@ZIF-8 nanospheres and the photocatalysis under UV irradiation. Matter. Letters. 2015;156:50-53: DOI: 10.1016/j.matlet.2015.04.142.

10. Wee LH, Janssens N, Sree SP, Wiktor C, Gobechiya E, Fischer RA, et al. Local transformation of ZIF-8 powders and coatings into ZnO nanorods for photocatalytic application. Nanoscale. 2014;6(4):2056-60: DOI: 10.1039/C3NR05289C.

11. Liu Q, Low Z-X, Li L, Razmjou A, Wang K, Yao J, et al. ZIF-8/Zn_2GeO_4 nanorods with an enhanced CO_2 adsorption property in an aqueous medium for photocatalytic synthesis of liquid fuel. Journal of Materials Chemistry A. 2013;1(38):11563-69: DOI: 10.1039/C3TA12433A.

12. Isimjan TT, Kazemian H, Rohani S, Ray AK. Photocatalytic activities of Pt/ZIF-8 loaded highly ordered TiO_2 nanotubes. Journal of Materials Chemistry. 2010;20(45):10241-245: DOI: 10.1039/C0JM02152K.

13. Chen L, Peng Y, Wang H, Gu Z, Duan C. Synthesis of Au@ZIF-8 single- or multi-core-shell structures for photocatalysis. Chemical Communications (Camb). 2014;50(63):8651-54: DOI: 10.1039/C4CC02818J.

14. Gao S-T, Liu W-H, Shang N-Z, Feng C, Wu Q-H, Wang Z, et al. Integration of a plasmonic semiconductor with a metal–organic framework: a case of Ag/AgCl@ZIF-8 with enhanced visible light photocatalytic activity. RSC Advances. 2014;4(106):61736-42: DOI: 10.1039/C4RA11364K.

15. Li R, Ren X, Ma H, Feng X, Lin Z, Li X, et al. Nickel-substituted zeolitic imidazolate frameworks for time-resolved alcohol sensing and photocatalysis under visible light. Journal of Materials Chemistry A. 2014;2(16):5724-29: DOI: 10.1039/C3TA15058E.

16. Demir NK, Topuz B, Yilmaz L, Kalipcilar H. Synthesis of ZIF-8 from recycled mother liquors. Microp. Mesoporus. Mat. 2014;198:291

Türkçe Öz ve Anahtar Kelimeler

Ag^+ Doplanmış ZIF-8 ve ZIF-L Kristallerinin Fotokatalitik Aktiviteleri

Hüsnü Arda Yurtsever, Melis Yağmur Akgünlü, Tuğçe Kurt, Ali Semih Yurttas,

Berna Topuz*

Öz: Zeolitik imidazolat yapısı (ZIF) esaslı metal organik yapı (MOF) fotokatalizörleri hazırlanmış ve ZIF-8 ile ZIF-L kristallerinin fotokatalitik aktivitelerine gümüş (Ag^+) doplamanın etkisi incelenmiştir. Ag^+ doplanmış ZIF-8 ve ZIF-L kristalleri hazırlanmış ve literatürde ilk kez UV ışıması altında metilen mavisinin (MB) fotokatalitik giderilmesinde kullanılmıştır. Doplanmış ZIF-8 ve ZIF-L kristalleri doplanmamış kristallerle karşılaştırıldığında daha iyi fotokatalitik aktivite göstermiştir. 40 dakika içinde 5 mol % Ag^+ ile doplanmış ZIF-8 ile neredeyse %100 MB giderilmiştir. Hesaplanan ikinci mertebe tepkime hız sabitlerinin büyüklüğü %5 > %10 > %2 > %1 > doplanmamış ZIF-8 sırasında değişmiştir. Fotokatalitik aktivite 5 mol % doplama seviyesinden sonra düşmüştür, çünkü Ag^+ iyonları, ZIF-8 örgüsü içinde belli bir katı hal çözünme sınırına ulaşmış olabilir. ZIF-L kristalleri ZIF-8 kristallerine oranla daha düşük fotokatalitik aktivite göstermiştir.

Anahtar kelimeler: Fotokataliz, metal organik yapı, ZIF-8, ZIF-L, doplama.

Gönderme: 4 Temmuz 2016. **Düzeltme:** 28 Temmuz 2016. **Kabul:** 01 Eylül 2016.